Heliyon 10 (2024) e33685

Contents lists available at ScienceDirect

Heliyon

journal homepage: www.cell.com/heliyon

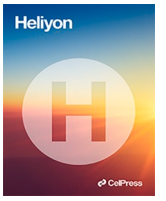

Research article

Biomechanical effects of different instrumented segments and trunk shifts on distal adjacent segments after congenital scoliosis posterior hemivertebrectomy: Preliminary results of a single case

Bei-xi Bao, Hui Yan, Jia-guang Tang *, Dao-jing Qiu, Yu-xuan Wu, Xiao-kang Cheng

Department of Orthopedic Surgery, Beijing Tongren Hospital, Capital Medical University, Beijing, 100730, China

ARTICLE INFO

Keywords:
Congenital scoliosis
Hemivertebra
Biomechanics
finite element analysis

ABSTRACT

Objective: The present study aims to discuss the biomechanical effects of the sagittal vertical axis and different instrumented segments on distal adjacent segments after congenital scoliosis posterior hemivertebrectomy.

Method: A case of congenital scoliosis caused by hemivertebra was selected for the reconstruction of the preoperative and postoperative 3D computed tomography data of the full spine. A finite element model of different fusion lengths and postoperative trunk shift (TS) values was established using the finite element method to compare the biomechanical effects of different models on the distal adjacent segment.

Result: In the L1–L3 and T12–L1–L3–L4 fusion modes, the horizontal shift of the 1st vertebra below the lowest instrumented vertebra (LIV) increased with the trunk shift (TS) expansion after operation, and the imbalance between the left and right vertical stress of the 1st intervertebral disc below the LIV increased. With the decrease in fused segments in cases of TS = 10 mm and TS = 5 mm, the 1st vertebra below the LIV was subjected to a greater unbalanced force in the horizontal direction, and the 1st intervertebral disc below the LIV was subjected to a smaller imbalance between the left and right vertical stress after operation.

Conclusion: When treating congenital scoliosis with hemivertebrectomy and pedicle screw fixation, fused segments can be properly extended and the postoperative TS shortened with a view of reducing the imbalance between the left and right stress of the 1st intervertebral disc below the LIV as well as the horizontal shift of the 1st vertebra below the LIV.

1. Background

Congenital scoliosis is a spinal deformity caused by unbalanced spinal growth; it accounts for approximately 10 % of all scoliosis deformities [1]. The prevalence of congenital vertebral deformity is approximately 0.5 ‰–1 ‰ among live-born infants, and this figure may be much lower than the real prevalence, as many child patients are asymptomatic [2]. The disease cause may be poor segmentation or formation defects of vertebra.

Hemivertebra is a congenital spinal deformity caused by defects in the formation of vertebra [3]; it is the chief culprit of congenital

* Corresponding author.
E-mail address: tangjiaguang2020@ccmu.edu.cn (J.-g. Tang).

https://doi.org/10.1016/j.heliyon.2024.e33685
Received 12 February 2023; Received in revised form 20 June 2024; Accepted 25 June 2024
Available online 27 June 2024

scoliosis. Currently, a range of surgical options are available for the treatment of congenital scoliosis caused by hemivertebra, including posterior decompression with instrumented in situ fusion, anterior and posterior combined decompression with instrumented in situ fusion, convex half epiphysiodesis [4], hemivertebrectomy [5], growing rod technique [6], vertical expandable prosthetic titanium rib [7,8], SHILLA [9], and growth-guided therapy.

Posterior hemivertebrectomy with short-segment fusion can deliver a desirable correction effect by providing stable fixation for a deformed spine. It is an effective surgical option in the treatment of congenital scoliosis caused by thoracolumbar hemivertebra. Even so, the operation may result in a series of postoperative complications, among which the distal adding-on phenomenon is a key manifestation of deformity progress in the wake of coronal surgery.

Severe cases with the phenomenon may require re-operation, with spines subjected to long-term negative impacts [10]. The diagnostic criteria for the distal adding-on phenomenon is the gradual increase in the number of vertebrae contained in the distal curvature; the shift of the central sacral vertical line of the 1st vertebra below the lowest instrumented vertebra (LIV) increases by > 5 mm, or the angle of the 1st intervertebral disc below the LIV increases by $> 5^{\circ}$ [11]. Therefore, the horizontal shift of the 1st vertebra below the LIV and the left–right stress difference of the 1st intervertebral disc below the LIV are the root causes of this complication.

In addition to the evaluation of geometric deformity, analysis of material and mechanical properties of the spine is also crucial for the study of scoliosis mechanism and treatment [12–14].

To date, the selection of scoliosis treatment relies largely on the experience of the surgeon. For this reason, patient-specific modeling tools are needed to help surgeons plan surgeries, intervene in and optimize treatment effects for patients, and predict postoperative complications. The combination of finite element modeling and experimental techniques has been employed in spine research for nearly half a century.

Spinal structures (such as vertebrae) can be divided into a collection of sub-parts in finite element modeling. Each sub-part can be represented by a limited number of elements interconnected with a shared node, and thus can accurately represent complex geometric structures. Besides, this method can also include different material properties and perform different types of analysis (e.g., static and dynamic analysis) [15–17]. Information that could not be measured through mechanical experiments, such as stress and strain, can be obtained based on these analyses.

The etiology of scoliosis, the biomechanics of curvature progression in the disease, and the effects of various implants on scoliosis surgery have been studied with different finite element models.

Until now, however, no biomechanical and finite element research has been carried out on the distal adjacent segments after posterior hemivertebrectomy with pedicle screw fixation. Therefore, through finite element modeling, the authors of the present study have attempted to analyze the effects of the sagittal vertical axis and different instrumented segments on the biomechanics of distal adjacent segments after congenital scoliosis posterior hemivertebrectomy based on the finite element models of one patient. This aims to provide surgeons with guidance in surgical planning and protect patients from the postoperative distal adding-on phenomenon and deformity progress.

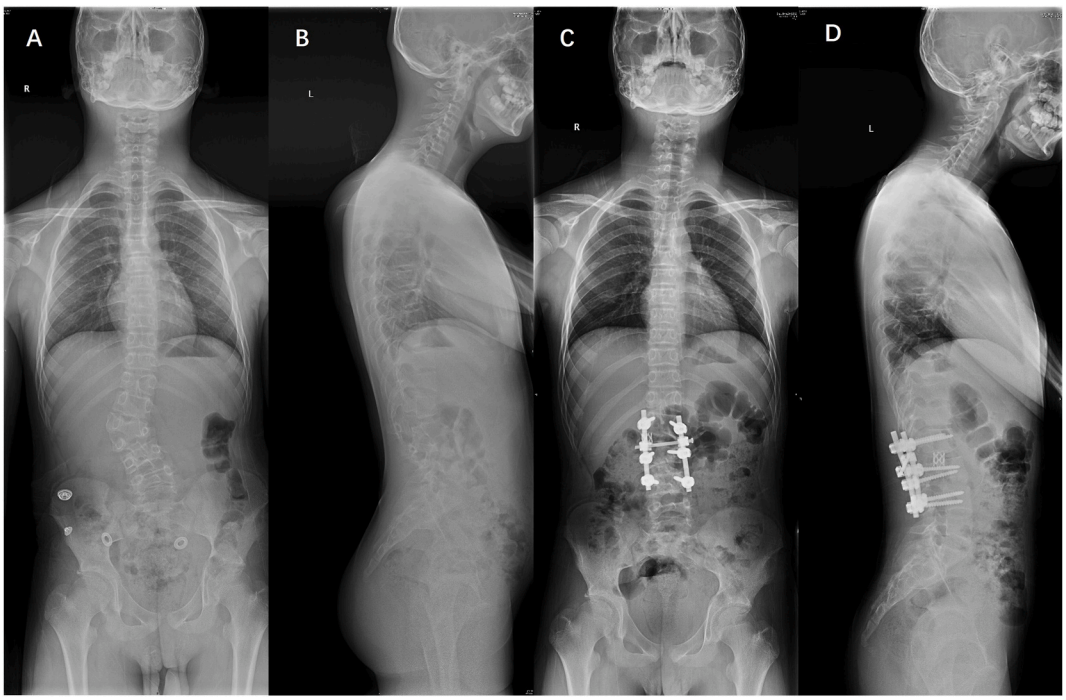

Fig. 1. Preoperative posterior-anterior (PA) & lateral (LAT) X-ray of the full spine (A, B): preoperative segmental scoliosis = 31.4°, TS = 25.4 mm. Postoperative PA & LAT X-ray of the full spine (C, D): postoperative segmental scoliosis = 12.8°, TS = 0 mm.

2. Method

A 12-year-old male patient with congenital scoliosis caused by hemivertebra was selected as the finite element model subject. The patient's hemivertebra was located in the L2 segment on the right side, with preoperative segmental scoliosis of 31.4° and TS of 25.4 mm. After operation, the segmental scoliosis was 12.8° and the TS was 0 mm (Fig. 1A–D).

Surgery: The patient was treated with posterior hemivertebrectomy and pedicle screw fixation. The patient was in the prone position in the wake of general anesthesia. A standard posterior median incision was made, and pedicle screws were respectively inserted into the proximal and distal vertebrae of the hemivertebra (L1, L3, and L4).

The titanium rod was subjected to pre-bending, connected to the pedicle screw at the convex side, and fixed temporarily.

Next, the convex side and transverse process of the L2 hemivertebra were resected, with the lateral and anterior hemivertebrae subjected to retroperitoneal blunt dissection. Rear structures of the hemivertebra and adjacent vertebrae, including the vertebral plate, zygapophyseal joints, and transverse processes, were removed via piezo surgery to expose and protect the pedicle and nerve roots.

The anterior vertebra was removed via wedge osteotomy using a rongeur, osteotome, curet, and drill. The upper and lower intervertebral discs, including cartilage endplates, were completely removed until the bleeding cancellous bone tissues were exposed. Anterior column reconstruction was completed by inserting titanium mesh into the L2 vertebra. At last, the convex side was pressurized and fixed, and the titanium rod was tightly locked.

Finite element modeling: The subject received a full spine computed tomography (CT) scan to obtain an image in the Dicom format with a spacing of 1 mm. The image was imported into Mimics to create a cone in the stereolithography (STL) format. The STL surface file was imported into Geomagic to obtain the NUEBS surface model, which was then converted into a computer-aided design model in the IGS format.

An intervertebral disc model was drawn using SolidWorks. A screw-rod model was established, and an assembly of the spine and screw-rod system was created based on the original coordinate of CT data. Finally, the model was subjected to finite element mesh division. Material properties were assigned to all components in HyperMesh to export an inp file as the final overall model.

Assignment of properties and element types: The material properties of cortical bone, cancellous bone, posterior element, and endplate were created in sequence. The main material properties were Young's modulus and Poisson's ratio. The material properties are shown in Table 1.

3. Result

A finite element model of different fusion lengths and postoperative TS values was established herein with the finite element method to compare the biomechanical effects of different models on a distal adjacent segment. In the present study, five finite element models were created: a C7–S1 preoperative hemivertebra finite element model, a 4-screw 2-rod L1–L3 fusion model (TS = 10 mm), a 4-screw 2-rod L1–L3 fusion model (TS = 5 mm), an 8-screw 2-rod T12–L1–L3–L4 fusion model (TS = 10 mm), and an 8-screw 2-rod T12–L1–L3–L4 fusion model (TS = 5 mm) (Fig. 2A–E).

4. .Effects of postoperative TS on the distal adjacent segment

Different postoperative TS values (TS = 10 mm and TS = 5 mm) with the same quantity of fused segments (4-screw 2-rod system and 8-screw 2-rod system) were simulated through the finite element model to observe the left–right stress difference of the 1st intervertebral disc below the LIV and the changes in the horizontal shift of the 1st vertebra below the LIV.

4.1. L1–L3 fusion (4-screw 2-rod)

When TS = 5 mm in the L1–L3 fusion finite element model, the horizontal shift of L4 was 0.6661 mm, and the left–right stress difference of the L34 intervertebral disc was 0.007 MPa. When TS = 10 mm, the horizontal shift of L4 was 0.7756 mm, and the left–right stress difference of the L3–4 intervertebral disc was 0.255 MPa. This indicates that in the L1–L3 fusion mode, the horizontal shift of the 1st vertebra below the LIV increases as the TS expands after operation, and the imbalance between the left and right vertical stress of the 1st intervertebral disc below the LIV increases (Fig. 3A–F).

Table 1
Material and section properties of each part of the finite element model.

Vertebra structure	Element type	Modulus of elasticity/MPa	Poisson's ratio
Cortical bone	Triangular shell element	12000	0.3
Cancellous bone	Tetrahedron element	150	0.3
Rear	Tetrahedron element	3500	0.3
Endplate	Triangular element	100	0.4
Vertebral pulp	Tetrahedron element	1	0.499
Fiber ring	Tetrahedron element	4	0.45
Pedicle screws	Tetrahedron element	110000	0.28
Connecting rod	Tetrahedron element	110000	0.28

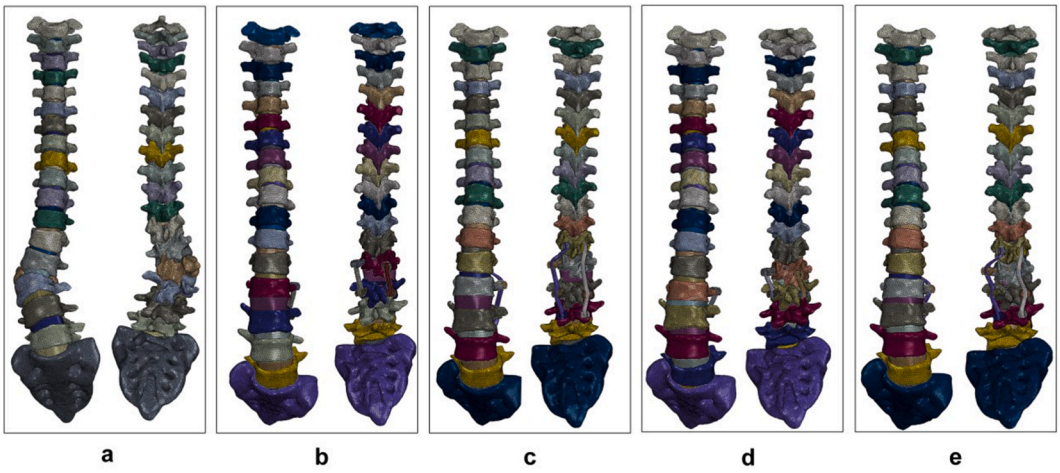

Fig. 2. Schematic diagram of preoperative and postoperative finite element model. A: Preoperative hemivertebra model; B: 4-screw 2-rod L1–L3 fusion model, TS = 10 mm; C: 8-screw 2-rod T12-L1-L3-L4 fusion model, TS = 10 mm; D: 4-screw 2-rod L1–L3 fusion model, TS = 5 mm; E: 8-screw 2-rod T12–L1–L3–L4 fusion model, TS = 5 mm.

4.2. T12–L1–L3–L4 fusion (8-screw 2-rod system)

In the T12–L1–L3–L4 fusion finite element model, when TS = 5 mm, the horizontal shift of L5 was 0.3805 mm, and the left–right stress difference of the L4–5 intervertebral disc was 2.198 MPa. When TS = 10 mm, the horizontal shift of L5 was 0.4483 mm, and the left–right stress difference of the L4–5 intervertebral disc was 3.041 MPa. This indicates that in the T12–L1–L3–L4 fusion mode, the horizontal shift of the 1st vertebra below the LIV increases as the TS expands after operation, and the imbalance between the left and right vertical stress of the 1st intervertebral disc below the LIV increases (Fig. 4A–F).

5. Effects of fusion methods on the distal adjacent segment

Different quantities of fused segments (4-screw 2-rod system and 8-screw 2-rod system) with the same postoperative TS value (TS = 10 mm and TS = 5 mm) were simulated through the finite element model to observe the left–right stress difference of the 1st intervertebral disc below the LIV and the changes in the horizontal shift of the 1st vertebra below the LIV.

5.1. TS = 10 mm

In the case of T12–L1–L3–L4 fusion in the finite element model with TS = 10 mm, the horizontal shift of L5 was 0.3805 mm, and the left–right stress difference of the L4–5 intervertebral disc was 3.041 MPa. In the case of L1–L3 fusion, the horizontal shift of L4 was 0.7756 mm, and the left–right stress difference of the L3–4 intervertebral disc was 0.255 MPa. This indicates that with a decrease in fused segments with TS = 10 mm, the 1st vertebra below the LIV records a greater horizontal shift, and the 1st intervertebral disc below the LIV shows a smaller imbalance between the left and right vertical stress after operation (Fig. 5A–F).

5.2. TS = 5 mm

In the case of T12–L1–L3–L4 fusion in the finite element model with TS = 5 mm, the horizontal shift of L5 was 0.4483 mm, and the left–right stress difference of the L4–5 intervertebral disc was 2.198 MPa. In the case of L1–L3 fusion, the horizontal shift of L4 was 0.6661 mm, and the left–right stress difference of the L3–4 intervertebral disc was 0.007 MPa. This indicates that with a decrease in fused segments when TS = 5 mm, the 1st vertebra below the LIV is subjected to a greater unbalanced force in the horizontal direction, and the 1st intervertebral disc below the LIV shows a smaller imbalance between the left and right vertical stress after operation (Fig. 6A–F).

6. Discussion

Congenital scoliosis is a spinal deformity caused by abnormal spinal growth, which is divided into poor segmentation and formation defects. Hemivertebra is the most common cause of congenital scoliosis, which can be treated with posterior hemivertebrectomy and pedicle screw fixation. However, postoperative complications, including the distal adding-on phenomenon and deformity progress, may occur. The distal adding-on phenomenon is characterized by the loss of a correction effect after scoliosis surgery, accompanied by progressive lumbar displacement and rotation as well as disc wedging at the distal end of the LIV.

Finite element modeling and simulation is a common research method in the field of spine biomechanics. Based on a CT scan of the

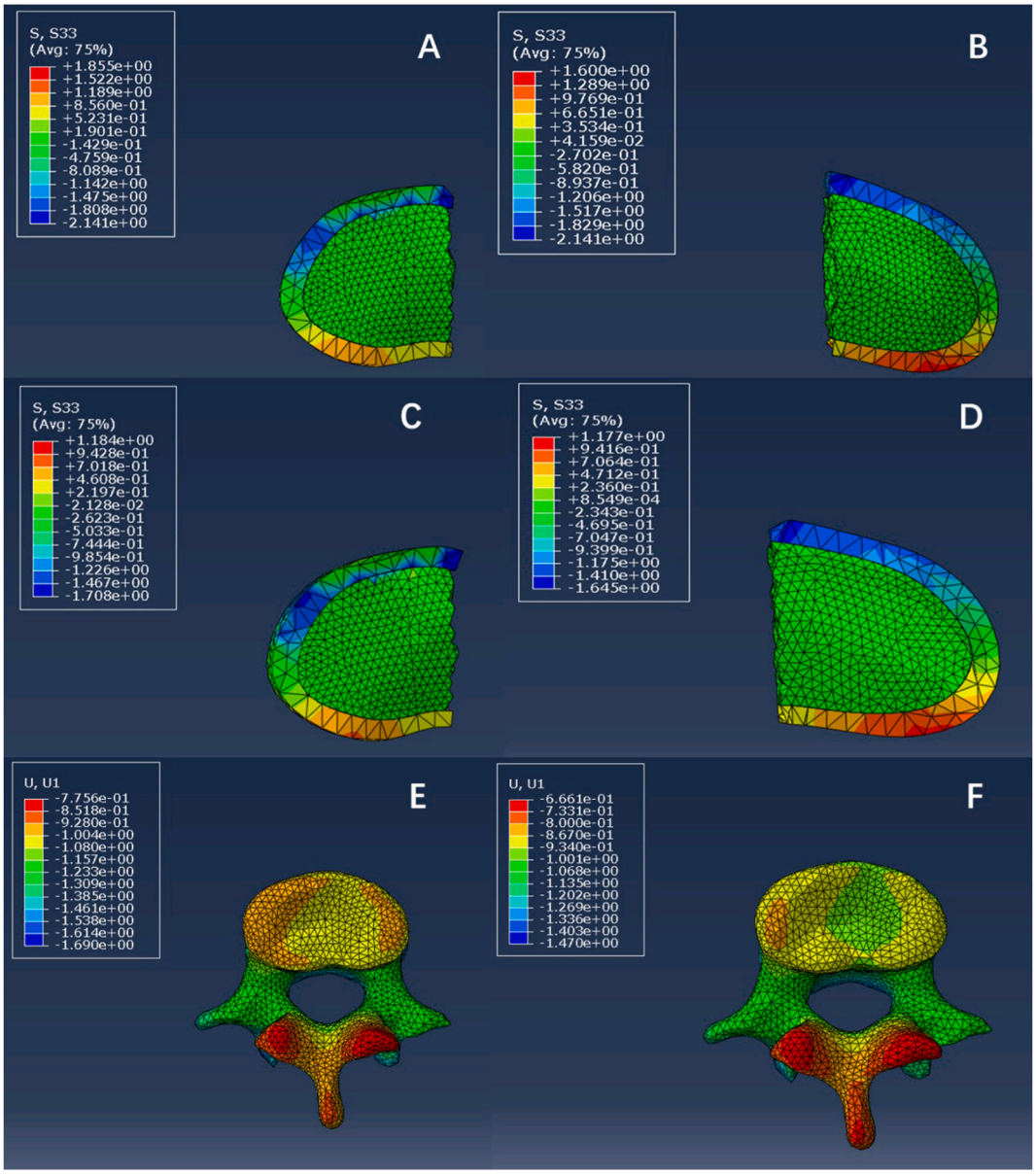

Fig. 3. The L1–L3 fusion finite element model. Stress distribution cloud diagram of the L3–4 intervertebral disc at the left (A) side and right (B) side when TS = 10 mm. Stress distribution cloud diagram of the L3–4 intervertebral disc at the left (C) side and right (D) side when TS = 5 mm. Horizontal shift of the L4 vertebra when TS = 10 mm (E) and TS = 5 mm (F).

patient's preoperative and postoperative spine shape, a numerical simulation model that is highly similar to the anatomical physiology of the real human body can be created using modeling and simulation software. By applying the same external loads as the real practice on the finite element model, the stress, shift, strain, and other information of each spinal segment, the intervertebral disc and pedicle screw can be obtained. In this way, the causes of external performance can be analyzed from the perspective of internal forces.

The surgical treatment of scoliosis mainly aims to enhance the coronal–sagittal balance, thus preventing further development of curvature. Based on a study by Yang et al. [18], postoperative coronal balance is a risk factor for postoperative adding-on phenomena in patients with Lenke Type 1 or 2 adolescent idiopathic scoliosis. According to the finite element research, when treating congenital scoliosis with posterior hemivertebrectomy and pedicle screw fixation, the horizontal shift of the 1st vertebra below the LIV increases as the TS expands after operation, and the imbalance between the left and right vertical stress of the 1st intervertebral disc below the LIV increases in the two fusion modes (L1–L3 fusion and T12–L1–L3–L4 fusion).

This indicates that the 1st vertebra below the LIV is more likely to exhibit horizontal movement as the TS expands after operation, while the 1st intervertebral disc below the LIV can cause different heights due to unbalanced forces and is thus more susceptible to disc wedging. For this reason, patients with a large TS after posterior hemivertebrectomy with pedicle screw fixation are more prone to

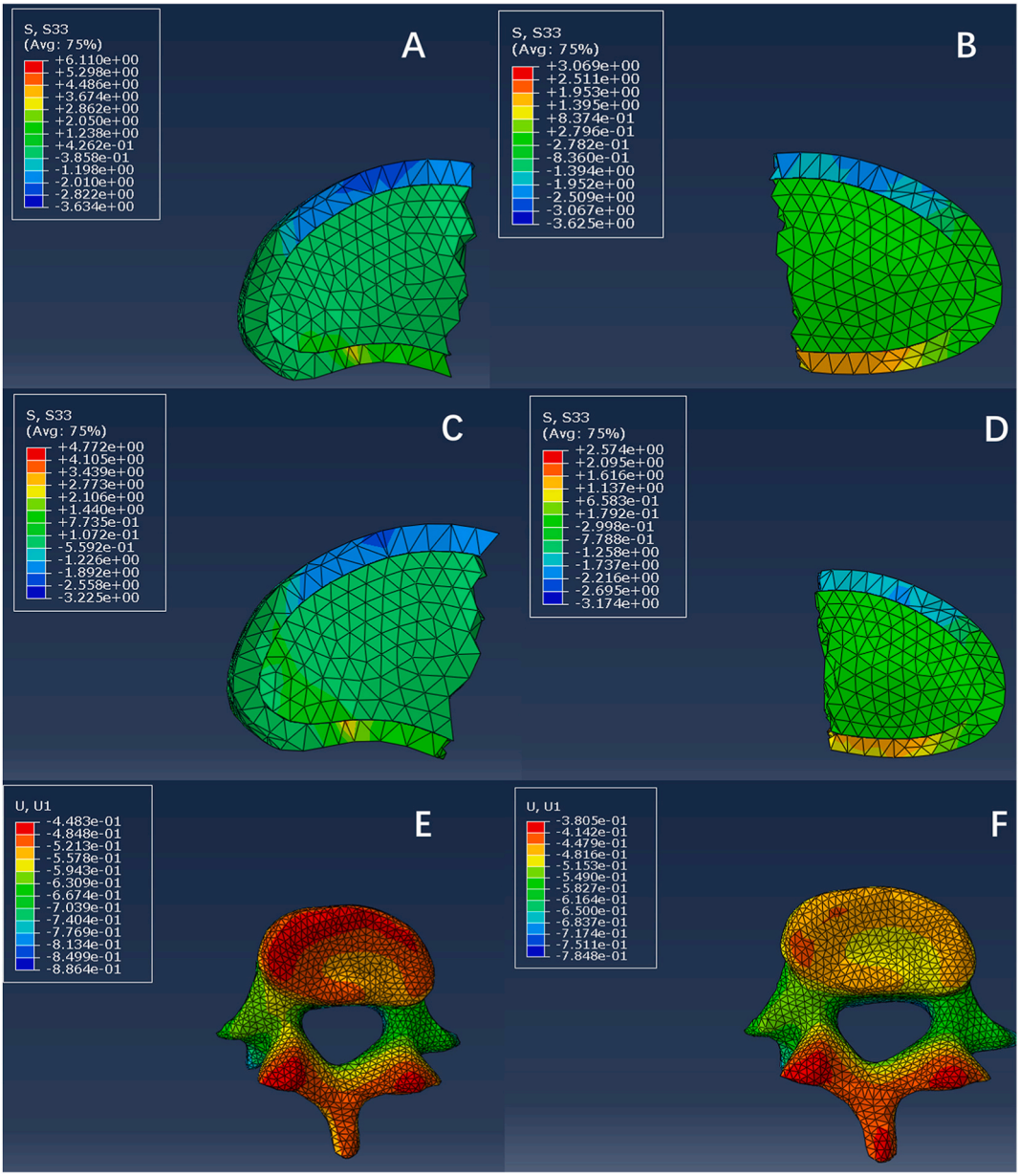

Fig. 4. The T12–L1–L3–L4 fusion finite element model. Stress distribution cloud diagram of the L4–5 intervertebral disc at the left (A) side and right (B) side when TS = 10 mm. Stress distribution cloud diagram of the L4–5 intervertebral disc at the left (C) side and right (D) side when TS = 5 mm. Horizontal shift of the L5 vertebra when TS = 10 mm (E) and TS = 5 mm (F).

losing the correction effect; this is accompanied by progressive lumbar displacement and rotation, as well as disc wedging at the distal end of the LIV.

Previous studies revealed that the occurrence of the distal adding-on phenomenon and deformity progress is closely relevant to the selection of instrumented segments in surgery. Based on the study by Ilharreborde and other scholars [19], although short-segment fusion achieves a good postoperative function score, the incidence of distal deformity progression is higher than that of long-segment fusion because the fused segment is short.

According to the finite element research, in the case of a decrease in fused segments with two postoperative TS values (TS = 10 mm and TS = 5 mm), the 1st vertebra below the LIV is subjected to a greater unbalanced force in the horizontal direction, and the 1st intervertebral disc below the LIV is subjected to a smaller imbalance between the left and right vertical stress after operation. This indicates that the effect of fewer fused segments on the 1st vertebra below the LIV is similar to that of a greater postoperative TS, which makes the horizontal movement more likely to happen.

With the decrease in fused segments, the imbalance between the left and right vertical stress of the 1st intervertebral disc below the

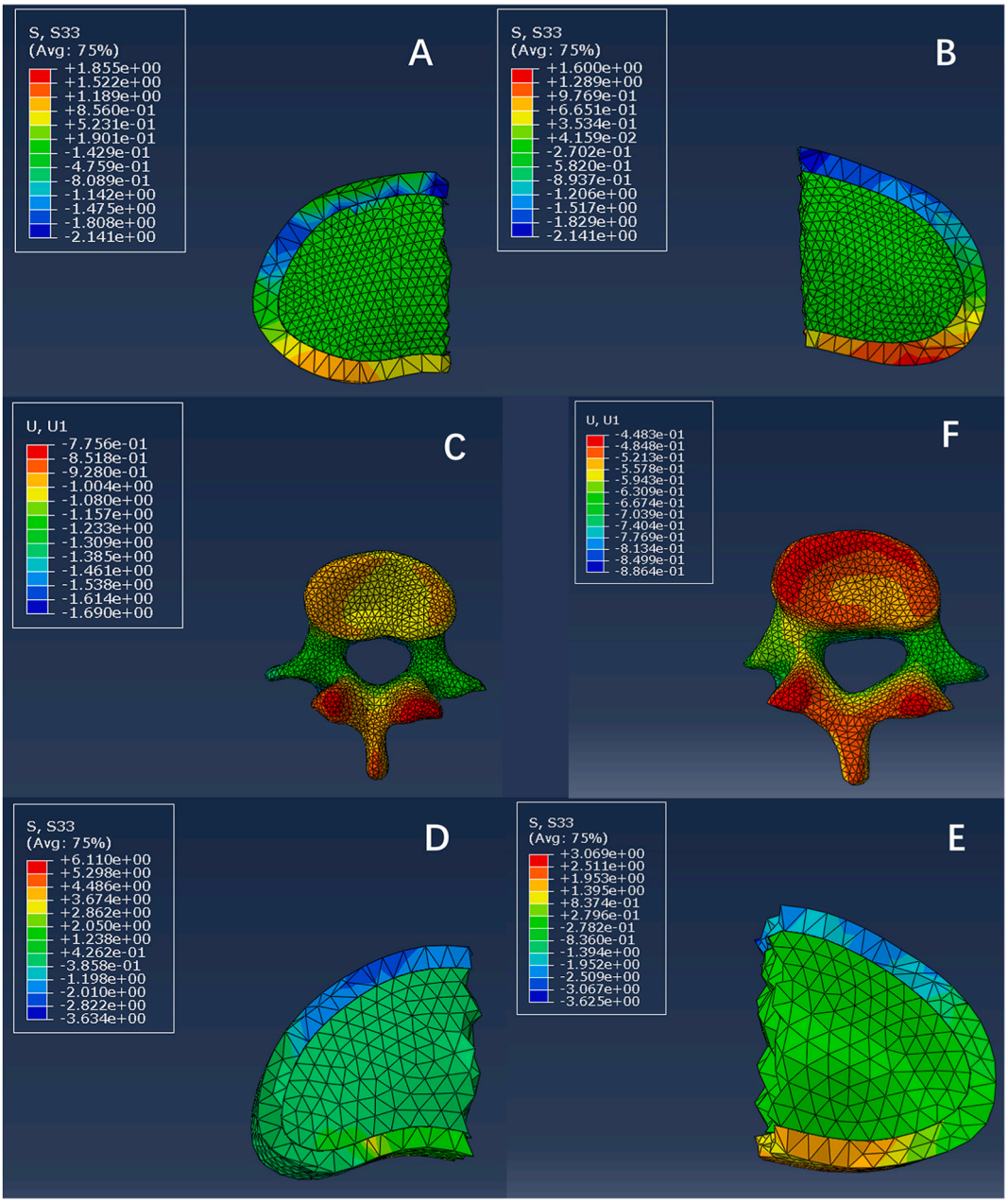

Fig. 5. Finite element model with TS = 10 mm. Stress distribution cloud diagram of the L3–4 intervertebral disc at the left (A) side and right (B) side in L1–L3 fusion. Horizontal shift (C) of the L4 vertebra in L1–L3 fusion. Stress distribution cloud diagram of the L4–5 intervertebral disc at the left (D) side and right (E) side in T12–L1–L3–L4 fusion. Horizontal shift (F) of the L5 vertebra in T12–L1–L3–βL4 fusion.

LIV becomes smaller, making the intervertebral disc more resilient to disc wedging. In this finite element research, however, the load was applied vertically downward on the upper surface of C7, remarkably affecting the vertical force of the intervertebral disc between segments.

Besides, as in the L1–L3 fusion model (4-screw 2-rod system), the 1st intervertebral disc below the LIV is L3–4, whereas in the T12–L1–L3–L4 fusion model (8-screw 2-rod system), the 1st intervertebral disc below the LIV is L4–5; the different intervertebral disc segments may cause inconsistent variables.

Even in a normal spine model, the left and right vertical stresses of L3–4 and L4–5 intervertebral discs also vary greatly. Based on this, the data results have a poor comparability, as it cannot be concluded that the smaller imbalance between the left and right vertical stress in L3–4 than in L4–5 in the present study is due to different intervertebral disc segments or different fused segments. In the L1–L3 fusion model (4-screw 2-rod system), the 1st vertebra below the LIV is L4; meanwhile, in the T12–L1–L3–L4 fusion model (8-screw 2-

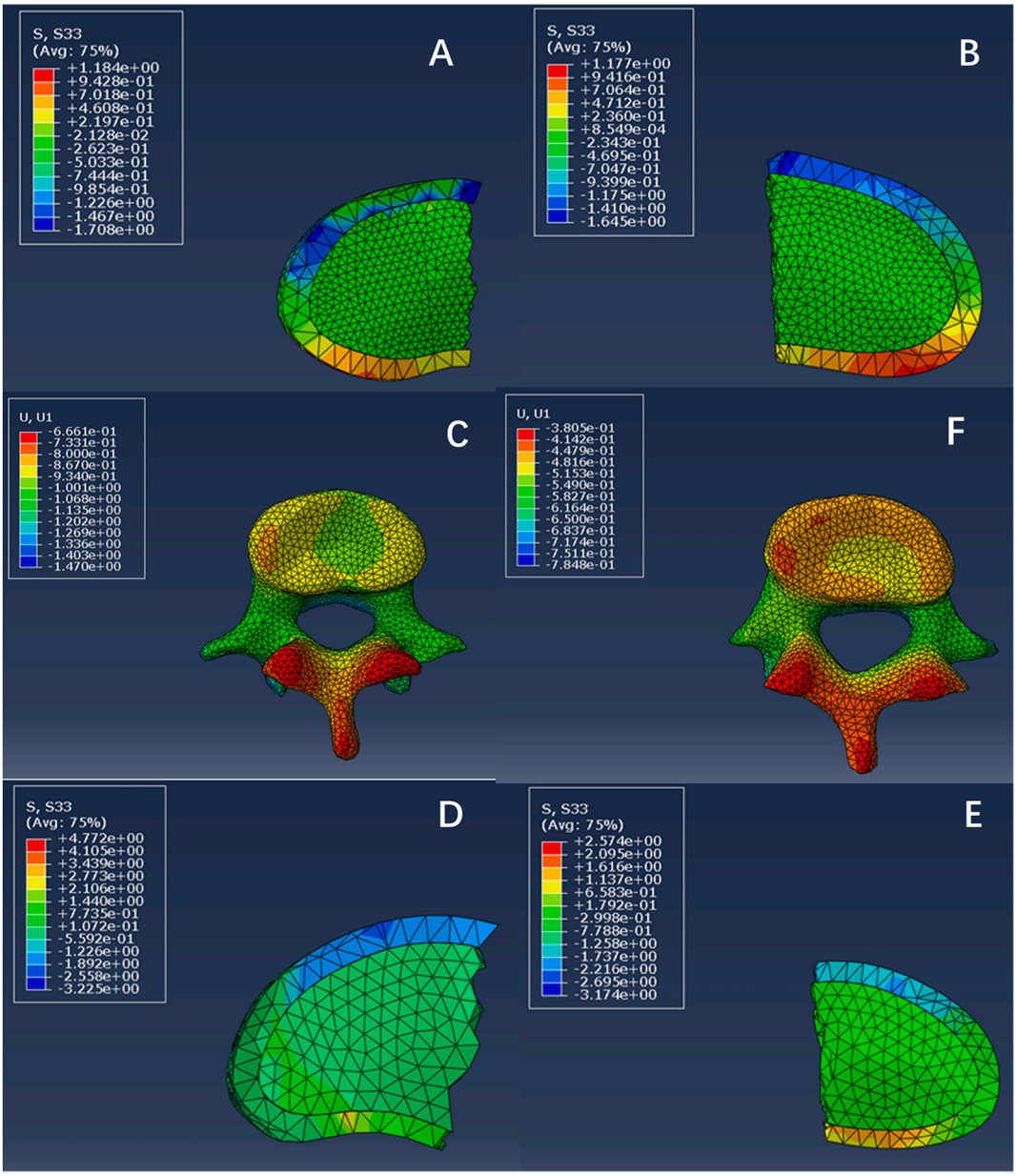

Fig. 6. Finite element model with TS = 5 mm. Stress distribution cloud diagram of the L3–4 intervertebral disc at the left (A) side and right (B) side in L1–L3 fusion. Horizontal shift (C) of the L4 vertebra in L1–L3 fusion. Stress distribution cloud diagram of the L45 intervertebral disc at the left (D) side and right (E) side in T12–L1–L3–L4 fusion. Horizontal shift (F) of the L5 vertebra in T12–L1–L3–L4 fusion.

rod system), the 1st vertebra below the LIV is L5.

As mentioned above, the variables are inconsistent. However, in contrast, the vertical loading has a smaller effect on the horizontal force. In a normal spine model, the difference in horizontal stress between the L4 and L5 vertebrae is very small, indicating that the different intervertebral disc segments will not affect the horizontal stress of the L4 and L5 vertebrae. Therefore, the smaller horizontal force in L4 than in L5 specified herein is due to the decrease in fused segments.

Finite element analysis certainly has its limitations. First, the finite element model is simplified and thus does not include all ligaments. In case of any slight change in the position of the simulated pedicle screw, the accuracy of the analysis will be affected. Second, the finite element model only represents the short-term preoperative and postoperative changes in this patient, and a dynamic follow-up observation was not carried out for him. Third, the real material properties of each component of the spine were not available in this finite element research; thus, the values thereof can only be assigned based on references.

7. Conclusion

According to the finite element analysis of our research, when posterior hemivertebra resection and pedicle screw fixation were used to treat congenital scoliosis, under two fusion methods (L1-L3 fusion and t12-l1-l3-l4 fusion), with the increase of postoperative trunk displacement distance, the horizontal displacement of the first vertebral body under the distal fixed vertebra increased, and the vertical stress imbalance between the left and right of the first intervertebral disc under the distal fixed vertebra increased. In two cases of postoperative trunk displacement distance (ts = 5 mm and ts = 10 mm), with the reduction of fusion segment, the horizontal imbalance of the first vertebral body under the distal fixed vertebra increases, and the vertical stress imbalance of the first intervertebral disc under the distal fixed vertebra decreases.

In conclusion, when treating congenital scoliosis with hemivertebrectomy and pedicle screw fixation, fused segments can be properly extended and the postoperative TS shortened with the view of reducing the imbalance between the left and right stress of the 1st intervertebral disc below the LIV as well as the horizontal shift of the 1st vertebra below the LIV. This is essential for protecting patients from the postoperative distal adding-on phenomenon and deformity progress.

Ethics approval and consent to participate

This study was conducted in accordance with the declaration of Helsinki.This study was conducted with approval on February 22, 2023 from the Ethics Committee of Beijing Tongren Hospital, Capital Medical University(TREC2024-KYS037). A written informed consent was obtained from participant.

Consent for publication

Consent for publication was obtained from patient whose data are included in this manuscript.

Availability of data and materials

Data will be made available on request.

Funding

Not applicable.

CRediT authorship contribution statement

Bei-xi Bao: Writing – original draft, Conceptualization. **Hui Yan:** Writing – review & editing, Supervision. **Jia-guang Tang:** Writing – review & editing, Conceptualization. **Dao-jing Qiu:** Resources, Data curation. **Yu-xuan Wu:** Resources, Data curation. **Xiao-kang Cheng:** Resources, Formal analysis.

Declaration of competing interest

The authors declare that they have no known competing financial interests or personal relationships that could have appeared to influence the work reported in this paper.

Acknowledgements

We are particularly grateful to all the people who have given us help on our article.

References

[1] K. Birnbaum, M. Weber, A. Lorani, et al., Prognostic significance of the Nasca classification for the long-term course of congenital scoliosis, Arch. Orthop. Trauma Surg. 122 (7) (2002) 383–389.
[2] R. Wynne-Davies, Congenital vertebral anomalies: aetiology and relationship to spina bifida cystica, J. Med. Genet. 12 (3) (1975) 280–288.
[3] R.B. Winter, J.E. Lonstein, O. Boachie-Adjei, Congenital spinal deformity, Instr. Course Lect. 45 (1996) 117–127.
[4] A.G. King, G.D. Macewen, W.J. Bose, Transpedicular convex anterior hemiepiphysiodesis and posterior arthrodesis for progressive congenital scoliosis, Spine 17 (8 Suppl) (1992) S291–S294.
[5] D.C. Holte, R.B. Winter, J.E. Lonstein, et al., Excision of hemivertebrae and wedge resection in the treatment of congenital scoliosis, J. Bone Jt. Surg. Am. Vol. 77 (2) (1995) 159–171.
[6] S. Wang, J. Zhang, G. Qiu, et al., Dual growing rods technique for congenital scoliosis: more than 2 years outcomes: preliminary results of a single center, Spine 37 (26) (2012) E1639–E1644.
[7] R.M. Campbell JR., B.M. Adcox, M.D. Smith, et al., The effect of mid-thoracic VEPTR opening wedge thoracostomy on cervical tilt associated with congenital thoracic scoliosis in patients with thoracic insufficiency syndrome, Spine 32 (20) (2007) 2171–2177.
[8] R. Dayer, D. Ceroni, P. Lascombes, Treatment of congenital thoracic scoliosis with associated rib fusions using VEPTR expansion thoracostomy: a surgical technique, Eur. Spine J. : official publication of the European Spine Society, the European Spinal Deformity Society, and the European Section of the Cervical Spine Research Society 23 (Suppl 4) (2014) S424–S431.

[9] R.E. Mccarthy, F.L. Mccullough, Shilla growth guidance for Early-Onset scoliosis: results after a Minimum of five Years of follow-up, J. Bone Jt. Surg. Am. Vol. 97 (19) (2015) 1578–1584.
[10] S.I. Suk, S.M. Lee, E.R. Chung, et al., Selective thoracic fusion with segmental pedicle screw fixation in the treatment of thoracic idiopathic scoliosis: more than 5-year follow-up, Spine 30 (14) (2005) 1602–1609.
[11] Y. Wang, E.S. Hansen, K. Hoy, et al., Distal adding-on phenomenon in Lenke 1A scoliosis: risk factor identification and treatment strategy comparison, Spine 36 (14) (2011) 1113–1122.
[12] L.G. Gilbertson, V.K. Goel, W.Z. Kong, et al., Finite element methods in spine biomechanics research, Crit. Rev. Biomed. Eng. 23 (5–6) (1995) 411–473.
[13] J.P. Little, C. Adam, Patient-specific computational biomechanics for simulating adolescent scoliosis surgery: Predicted vs clinical correction for a preliminary series of six patients, Commun. Numer. Methods Eng. 27 (9) (2011) 347–356.
[14] H. Azegami, S. Murachi, J. Kitoh, et al., Etiology of idiopathic scoliosis. Computational study, Clin. Orthop. Relat. Res. 357 (1998) 229–236.
[15] C.E. Aubin, Y. Petit, I.A. Stokes, et al., Biomechanical modeling of posterior instrumentation of the scoliotic spine, Comput. Methods Biomech. Biomed. Eng. 6 (1) (2003) 27–32.
[16] C.E. Aubin, V. Goussev, Y. Petit, Biomechanical modelling of segmental instrumentation for surgical correction of 3D spinal deformities using Euler-Bernoulli thin-beam elastic deformation equations, Med. Biol. Eng. Comput. 42 (2) (2004) 216–221.
[17] Y. Majdouline, C.E. Aubin, A. Sangole, et al., Computer simulation for the optimization of instrumentation strategies in adolescent idiopathic scoliosis, Med. Biol. Eng. Comput. 47 (11) (2009) 1143–1154.
[18] C. Yang, Y. Li, M. Yang, et al., Adding-on phenomenon after surgery in Lenke type 1, 2 adolescent idiopathic scoliosis: is it predictable? Spine 41 (8) (2016) 698–704.
[19] B. Ilharreborde, E. Ferrero, A. Angelliaume, et al., Selective versus hyperselective posterior fusions in Lenke 5 adolescent idiopathic scoliosis: comparison of radiological and clinical outcomes, Eur. Spine J. : official publication of the European Spine Society, the European Spinal Deformity Society, and the European Section of the Cervical Spine Research Society 26 (6) (2017) 1739–1747.